CHIN. PHYS. LETT. Vol. 32, No. 6 (2015) 064202

# Probing of Ultrafast Plasmon Dynamics on Gold Bowtie Nanostructure Using Photoemission Electron Microscopy *

QIN Jiang(秦将)[1], JI Bo-Yu(季博宇)[1], HAO Zuo-Qiang(郝作强)[1**], LIN Jing-Quan(林景全)[1,2**]

[1]*School of Science, Changchun University of Science and Technology, Changchun 130022*

[2]*International Research Center for Nano Handling and Manufacturing of China, Changchun 130022*

(Received 7 February 2015)

*We report the direct imaging of plasmon on the tips of nano-prisms in a bowtie structure excited by 7 fs laser pulses and probing of ultrafast plasmon dynamics by combining the pump-probe technology with three-photon photoemission electron microscopy. Different photoemission patterns induced by the plasmon effect are observed when the bowties are excited by s- and p-polarized femtosecond laser pulses. A series of images of the evolution of local surface plasmon modes on different tips of the bowtie are obtained by the time-resolved three-photon photoemission electron microscopy, and the result discloses that plasmon excitation is dominated by the interference of the pump and probe pulses within the first 13 fs of the delay time, and thereafter the individual plasmon starts to oscillate on its own characteristic resonant frequencies.*

*PACS:* 42.65.Re, 68.37.Xy, 78.47.J−, 78.67.Bf DOI: 10.1088/0256-307X/32/6/064202

In recent years, ultrafast plasmon, which can be realized by concentrating femtosecond laser pulses in a subwavelength structure, has been intensively explored[1−4] and it has the potential to fabricate the plasmonic chip with speed in the peta-hertz domain.[5] Also, femtosecond plasmon offers the ability to perform ultrafast near field optical control and nano-optical switching.[6−12] To observe and characterize ultrafast plasmon and to explore methods for their control, a technique is needed that is capable of imaging the ultrafast plasmon with nanometer and femtosecond spatiotemporal resolution.

Femtosecond laser-based multiple-photon photoemission electron microscopy (PEEM) provides such capabilities. PEEM technology is used to observe a sample in a vacuum by forming two-dimensional intensity maps using electrons emitted from the sample surface, and thus it can offer images of nanostructures at electron resolution. Reports have shown that PEEM is a suitable tool for the imaging of localized optical field excited by femtosecond laser pulses.[13] Moreover, the PEEM technology reflects the actual distribution of the optical near field and involves no physical probe altering the measure, which could happen by using other probe-based near field measurement technologies such as scanning near field microscopy (SNOM) or related methods.[14−21] Therefore, a promising route to non-invasively unfold the ultrafast plasmon field is to combine PEEM with the femtosecond pump-probe technique, i.e., interferometric time-resolved photoemission electron microscopy (TR-PEEM).

With a photon energy of 1.55 eV of the Ti:sapphire femtosecond laser, a nonlinear photoemission process is necessary to overcome the work function of the metal. Time-resolved two photon PEEM with the second-harmonic emission of the laser has been successfully used in the imaging of spatiotemporal focusing of surface plasmon wave packets by the planar plasmonic-lens coupling silver structure,[22] and it has been demonstrated to the imaging and quantum control of surface plasmon dynamic in a nanostructured silver film.[23] As the photoelectron yield is proportional to the $2n$-th power of the local electric field, where $n$ is the order of the nonlinearity,[24] an adoption of three-photon PEEM (3P-PEEM) with the fundamental wavelength of the Ti:sapphire femtosecond laser will bring an advantage of more sensitive detection of LSP in a nanostructure over the case of the two-photon PEEM.[25] Moreover, reinforced with femtosecond interferometric time-resolved measurement, the TR-3P-PEEM technology is expected to unfold the plasmon field with high spatial and temporal resolution. On the other hand, for plasmon research, the gold bowtie is a typical and important nanostructure that has been used for a long period.[26−29] Especially in recent years, there is an increasing interest in the plasmon excitation of the gold bowtie by an ultrafast laser.[30,31] Up to now, there has been no report on imaging of ultrafast dynamics of LSP on the gold bowtie by the TR-3P-PEEM technology.

In this Letter, we report direct imaging of plasmon on the tips of the nano-prism in a bowtie structure excited by a 7 fs laser and probing of the femtosecond plasmon dynamic by using TR-3P-PEEM. We obtain

*Supported by the National Basic Research Program of China under Grant No 2013CB922404, the National Natural Science Foundation of China under Grant Nos 11474040 11274053, 11474039 and 61178022, and the Project under Grant No 14KP007.

**Corresponding author. Email: zqhao@cust.edu.cn; linjingquan@cust.edu.cn

© 2015 Chinese Physical Society and IOP Publishing Ltd

PEEM images of plasmon on the structure excited by p- and s-polarized femtosecond laser pulses. Based on the observation of local electric field enhancement on the tips of nano-prisms with a p-polarization laser, we further report the imaging of ultrafast dynamic evolution of the LSP modes on the gold bowtie by the TR-3P-PEEM technology at a temporal precision of 330 as.

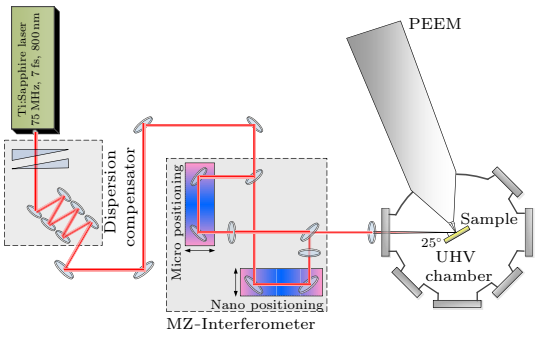


**Fig. 1.** Schematic diagram of the experimental setup consisting of a femtosecond Ti:sapphire laser system, a dispersion compensator, a high resolution MZ-Interferometer and a UHV-chamber with a PEEM.

Figure 1 shows a scheme of the experimental setup used in this study. The photoemission electron microscope (IS PEEM, Focus GmbH) with a lateral resolution of better than 40 nm is used to take the image of the LSP.[32] Two excitation sources are equipped for the PEEM experiment. One is a conventional unpolarized Hg lamp with a cutoff energy of 4.9 eV, and the other is a commercial Ti:sapphire laser oscillator at a central wavelength of 800 nm with a spectral bandwidth extending from 600–900 nm (FEMTOLASERS; Rainbow, 75 MHz repetition, 7 fs pulse width, 4 nJ pulse energy). As shown in Fig. 1, the light source illuminates the sample at an incident angle of 65° to the surface normal of the sample. The sample used in this study is a gold bowtie nanoantenna array, which is fabricated by electron beam lithography and a lift-off process. The gold bowtie structure is on top of a conductive indium tin oxide (ITO) film coated on a glass substrate. Figure 2 shows the scanning electron microscopy (SEM) image of a typical gold bowtie structure in the array.

The typical work function of the investigated gold nanostructure is about 4.7 eV,[33] and the cutoff photon energy of the Hg lamp is about 4.9 eV, photoelectron emission is one photon process when the bowtie is illuminated by the Hg lamp. In the experiment, s- and p-polarized femtosecond laser pulses are employed to excite the plasmon on the bowtie nanostructure, and polarization direction of the laser is changed using a half wavelength plate. In the experiment, the light beam from the Hg lamp and the femtosecond laser (s- and p-polarization) enter the PEEM chamber via different view ports and can be easily overlapped through adjustment to illuminate the same area of the sample. Even though images are taken with different excitation sources, the field of view of the PEEM reflects exactly the same point as long as the sample position is fixed and images are recorded with identical settings of PEEM electron optics. To investigate the plasmon dynamic of the bowtie, time-resolved experiments are realized in a pump-probe configuration using a Mach–Zehnder type interferometer. Here the femtosecond light is split into two pulses of equal intensity with the same polarization where a piezo-control optical delay line stage is employed to temporally delay one pulse with respect to the other. The resolution of the piezo-control stage is about 25 nm, which corresponds to a temporal delay of 167 as between the respective laser pulses through the different arms of interferometer. This allows one to map the local field distribution at the surface induced by the 800 nm light with the interferometric resolution. In our experiment a series of 3P-PEEM images were recorded at a frame interval of 330 as ($\pi/4$ rad with respect to the 800 nm carrier wave of the laser pulse) by adjusting the delay time $\tau_{\rm d}$, which is advanced from 0 to 44 fs. This corresponds to the relative phase change from 0 to $16 \times 2\pi$. Due to the fact that the laser pulse is short with a duration of 7 fs, the entrance window of the vacuum chamber of the PEEM and transmitted optical components in the interferometer will induce dispersion of the light pulse, thus a pair of chirp mirrors and two optical wedges are used in the beam path to compensate for the optical dispersion and to obtain the minimal pulse duration at the sample position.

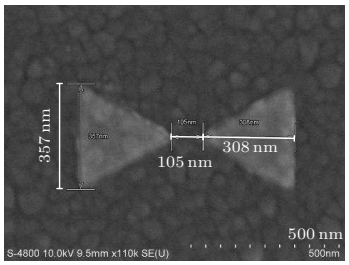


**Fig. 2.** Scanning electron microscopic image of the bowtie nanostructure. The parameters of the gold bowtie nanoantenna used in this study are taken as a prism with a side length of 357 nm, a gap of 105 nm between the two prisms and a thickness of 40 nm.

Figure 3(a) shows the one-photon photoemission image (1P-PEEM) excited with the continuous UV light (an Hg lamp). It clearly shows that two homogenously bright triangles, which correspond to high photoelectron yield, appear in the PEEM image, and they represent the two gold nano-prisms in the bowtie. The rest of the dark area in the image, which gives a low photoelectron yield, is from the ITO substrate of

the sample. Under the illumination of the Hg lamp source, a good contrast is obtained between the gold bowtie and the ITO substrate in the PEEM image. Figures 3(b) and 3(c) show the 3P-PEEM images of the bowtie excited with the p- and s-polarized femtosecond lasers, respectively. Figure 3 shows that there is a striking difference between the PEEM images obtained with one photon and three-photon processes. The 3P-PEEM images in Figs. 3(b) and 3(c) are recorded with identical setting of the PEEM electron optics as that of the 1P-PEEM case in Fig. 3(a), thus the scaling in 1P-PEEM and 3P-PEEM images is the same, which allows us to determine the position of the highly localized bright spots in the 3P-PEEM image. It is necessary to mention that the PEEM images in Figs. 3(a)–3(c) were taken while the sample position was un-shifted and all with the identical setting of the PEEM electron optics, which ensures that exactly the same area of the sample is imaged by the three excitation sources. Therefore, according to the 1P-PEEM image, we mark the contours of the nanoprisms, those are hard to distinguish in the 3P-PEEM image directly. From the 3P-PEEM images it is interesting to note that the surface of the two nanoprisms in the gold bowtie does not show homogenously bright anymore, instead highly localized bright spots (hotspots) are observed mostly on the edge of the nanoprisms.

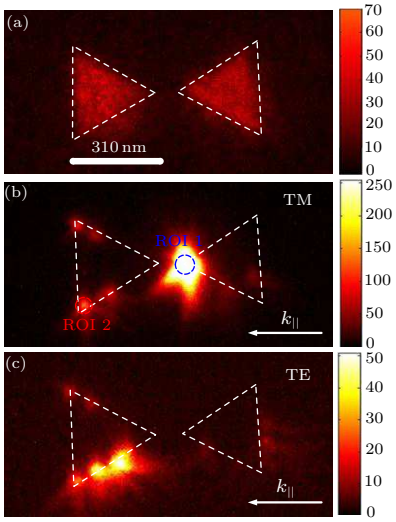


**Fig. 3.** PEEM images of a bowtie nanoantenna taken with different excitation sources (field of view: 2 μm ). (a) PEEM image taken with a UV lamp; (b) and (c) the same nanoprisms as in panel (a) illuminated by p- and s-polarized femtosecond laser pulses, respectively. Dashed lines are drawn to mark contours of the gold nanoprisms in the figure. The parallel component of the incident light wave vector is directed toward the left in our experiments.

Figure 3(b) shows that the most intense hot spot of photoelectron emission, which is marked by a blue circle and named as region of interest (ROI) 1, is centered at the tip of the right nanoprism under p-polarized (TM-polarization) femtosecond laser pulse excitation. Meanwhile, two weaker emission maxima (marked with red lines in the PEEM image) at the two outer corners of the left nanoprism are observed, and the lower one is marked as ROI 2. Furthermore, close to the two outer corners of the left nanoprism, there are some weaker bright spots appearing in the image. The bright spots in ROIs 1 and 2, including those observed close to the outer corners in the PEEM images, are caused by local electric field enhancement, namely a plasmon effect, they correspond to the enhanced photoelectron yield. The main reason for this asymmetry excitation of the plasmon phenomenon in the bowtie is attributed to the retardation effect, which occurs under conditions that the structure size under study is on the order of wavelength of the oblique incident of the laser pulse.[34] A full explanation of the mechanism of ROIs 1 and 2 formation in this grazing incidence illumination configuration needs more theoretical work. However, a similar result showing asymmetric excitation of plasmon phenomenon on bowtie under grazing incidence illumination was previously observed in a PEEM experiment and has been well reproduced by simulation.[8]

Figure 3(c) shows the PEEM image obtained with the s-polarized (TE-polarization) light excitation. The laser intensity is the same as that of the TM excitation case. It is seen that there is a significant difference in the photoelectron emission pattern when the excitation laser is changed from p- to s-polarization. In Fig. 3(c) we could hardly see any photoemission from the tips of the nanoprism in the bowtie. Moreover, bright spots at two corners of the left prism are weakly pronounced with a lower photoelectron yield compared with the case of under p-polarized light excitation. However, the bright spots close to the ROI 2 on the left nanoprism become more intense than those observed with p-polarization laser illumination. Evidently, Figs. 3(b) and 3(c) indicate that both the intensity and location of hotspots depend sensitively on the polarization state of the incident light.

It is noted that the bright spots, appearing not on the tips or the outer corners of the nanoprisms in the PEEM images of Figs. 3(b) and 3(c), are some unexpected spots, and they mainly located at the edge region of the gold bowtie nanostructures. The most likely reason responsible for their appearance is that the bright spots are caused by random structures existing in the edge region on the sample surface. Indeed, the protrusions and irregularities will inevitably be generated during the sample preparation process and they easily occur in the edge region of the structure. When the random structures are excited by wide bandwidth (ranging from 600 nm to 900 nm) femtosec-

ond laser pulses, the LSP wavelengths of some protrusions and irregularities overlap with the laser spectrum, resulting in plasmon excitation. Another possible reason is that a lightning rod effect compresses the electric field at the edges into these protrusions, leading to some of the areas appearing to be bright.[35]

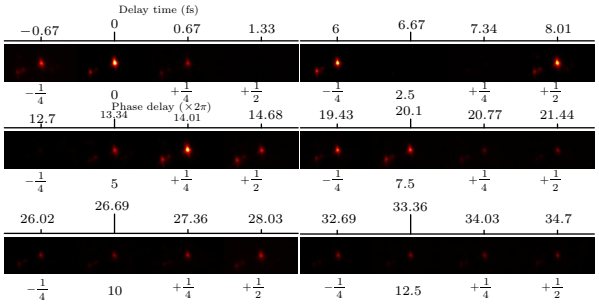


**Fig. 4.** Selected TR-3P-PEEM images at different delay times for a gold bowtie nanostructure. The delay time between pump and probe pulses is advanced from −0.67 fs to 34.7 fs in terms of the optical phase of the carrier light with an increment step of 0.67 fs.

In the following experiment, time-resolved-3P-PEEM is used to investigate the ultrafast plasmon dynamic of the bowtie nanostructure under the p-polarized light excitation with a temporal interval of 330 as between the pump and probe laser pulses. A series of PEEM images at various delay times is shown in Fig. 4. The PEEM images show that the brightness of the hot spots at the ROIs 1 and 2 on the bowtie sample has a periodical oscillation when the delay time is shorter than 32 fs, i.e., the two hot spots switch on and off regularly with a delay time. In a late stage, as seen from four images from the figures in the last row of the right panel, the images show that two regions are almost with no change in the brightness.

To further quantitatively clarify the phase evolution of these two regions, integrated intensity of the three-photon photoemission signal of each spot versus the delay time is plotted in Fig. 5. As seen from the right-top panel of Fig. 5, the relative phase of the photoemission from ROIs 1 and 2 is zero when the delay time is shorter than 13 fs. As time goes on, on the intermediate time scales (13 fs$\leq \tau_{\rm d} \leq$32 fs), the phase response of ROI 2 has been significantly delayed with respect to ROI 1. On the much longer time scales ($\tau_{\rm d} >$ 32 fs), the phase delay between two regions can hardly be distinguished due to the weakening of the photoelectron emission. Evolution of the two plasmon phase with the delay time can be explained in the following. At the beginning of the excitation, the interference of the pump and probe pulses dominates the oscillation of the LSP and forces them to resonate at the laser frequency. As the delay time increases, the pump and probe pulses are separated (no longer overlap), the coherently excited LSP fields can still retain the memory of the phases of the pump pulse and the probe pulse, leading to the interference between the pump and probe induced LSP fields, thus the hot spots are still oscillating. However, each hot spot oscillates at its own characteristic resonance frequency. This is due to the fact that in our case, the polarization direction of the excitation light field is along the horizontal direction of the bowtie antenna (see Fig. 3(b)); the tip in ROI 1 and the outer corner in ROI 2 show many different respects related to the excitation light field, and this makes the difference from plasmon resonance, giving rise to plasmon eigenfrequency of the two regions that are not identical. As a result, the relative phase of the two regions is not zero starting from the intermediate time scale (from $\tau_{\rm d} >$ 13 fs, see the lower right panel). Moreover, we find that it is impossible to see any oscillation of the hot spots due to the fact that the pump and probe pulse induce weak photoemission signals independently. Note that the polarization-dependent excitation and the ultrafast plasmon dynamic behavior of corners of the nanoprism under a femtosecond laser illumination observed in this experiment are uniform results, which is applied to each nanoprism in the array.

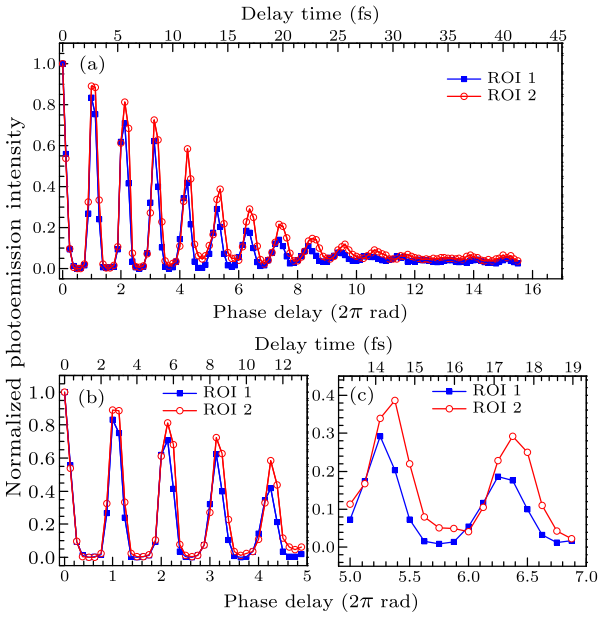


**Fig. 5.** (a): Evolution of the photoemission signals with a delay time. (b,c): Two magnified regions.

The switch-on and switch-off plasmon resonances as demonstrated in the experiment suggest that the local optical field can be controlled at will by changing the delay time between the two pulses, and the control of local optical field distribution can be realized at nanometric and femtosecond spatiotemporal resolution. This opens the way for the applications of ultrafast plasmon such as in the field of ultrafast

optical switching or optical logic calculation.

We thank Professor Toshihisa Tomie for the useful discussion.

## References

[1] Brinks D, Castro-Lopez M, Hildner R and Hulst N F 2013 *Proc. Natl. Acad. Sci. USA* **110** 18386
[2] MacDonald K F, S ámson Z L, Stockman M I and Zheludev N I 2009 *Nat. Photon.* **3** 55
[3] Rewitz C, Keitzl T, Tuchscherer P, Huang J S, Geisler P, Razinslas G, Hecht B and Brixner T 2012 *Nano Lett.* **12** 45
[4] Utikal T, Stockman M I, Heberle A P, Lippitz M and Giessen H 2010 *Phys. Rev. Lett.* **104** 113903
[5] http://www.bacatec.de/en/gefoerderte_projekte.html
[6] Stockman M I, Sergey V F and David J B 2002 *Phys. Rev. Lett.* **88** 067402
[7] Brixner T, de Abajo F G, Schneider J and Pfeiffer W 2005 *Phys. Rev. Lett.* **95** 093901
[8] Melchior P, Bayer D, Schneider C, Fischer A, Rohmer M, Pfeiffer W and Aeschlimann M 2011 *Phys. Rev.* B **83** 235407
[9] Zherebtsov S, Fennel T, Plenge J et al 2011 *Nat. Phys.* **7** 656
[10] Könenkamp R, Word R C, Fitzgerald J P S, Nadarajah A and Saliba S D 2012 *Appl. Phys. Lett.* **101** 141114
[11] Word R C, Fitzgerald J P S and Könenkamp R 2014 *Appl. Phys. Lett.* **105** 111114
[12] Rewitz C, Razinskas G, Geisler P et al 2014 *Phys. Rev. Applied* **1** 014007
[13] Cinchetti M, Gloskovskii A, Nepjiko S A, Schönhense G, Rochholz H and Kreiter M 2005 *Phys. Rev. Lett.* **95** 047601
[14] Grubisic A, Ringe E, Cobley C M, Xia Y, Marks L D, Van Duyne R P and Nesbitt D J 2012 *Nano Lett.* **12** 4823
[15] Schweikhard V, Grubisic A, Baker T A, Thomann I and Nesbitt D J 2011 *ACS Nano* **5** 3724
[16] Imura K, Tetsuhiko N and Hiromi O 2005 *J. Phys. Chem.* **122** 154701
[17] Imura K, Ueno K, Misawa H and Okamoto H 2011 *Nano Lett.* **11** 960
[18] Rang M, Jones A C, Zhou F, Li Z Y, Wiley B J, Xia Y N and Raschke M B 2008 *Nano Lett.* **8** 3357
[19] Tanaka Y, Ishiguro H, Fujiwara H, Yokota Y, Ueno K, Misawa H and Sasaki K 2011 *Opt. Express* **19** 7726
[20] Ueno K, Juodkazis S, Mizeikis V, Sasaki K and Misawa H 2008 *Adv. Mater.* **20** 26
[21] Imura K, Okamoto H, Hossain M K and Kitajima M 2006 *Nano Lett.* **6** 2173
[22] Wang L M and Hrvoje P 2013 *Laser Photon. Rev.* **7** 1003
[23] Kubo A, Onda K and Petek H 2005 *Nano Lett.* **5** 1123
[24] Merschdorf M, Kennerknecht C and Pfeiffer W 2004 *Phys. Rev.* B **70** 193401
[25] Sun Q, Ueno K, Yu H et al 2013 *Light: Sci. Appl.* **2** e118
[26] Schuck P J, Fromm D P, Sundaramurthy A, Kino G S and Moerner W E 2005 *Phys. Rev. Lett.* **94** 017402
[27] Kim S, Jin J, Kim Y J, Park I Y, Kim Y and Kim S W 2008 *Nature* **453** 757
[28] Kinkhabwala A, Yu Z, Fan S, Avlasevich Y, Müllen K and Moerner W E 2009 *Nat. Photon.* **3** 654
[29] Gramotnev D K, Pors A, Willatzen M and Bozhevolnyi S I 2012 *Phys. Rev.* B **85** 045434
[30] Hanke T, Krauss G, Träutlein D, Wild B, Bratschitsch R and Leitenstorfer A 2009 *Phys. Rev. Lett.* **103** 257404
[31] Kollmann H, Piao X, Esmann M et al 2014 *Nano Lett.* **14** 4778
[32] Focus PEEM http://www.omicron.de/en/products/focus-peem-/instrument-concept
[33] Riviere J C 1966 *Appl. Phys. Lett.* **8** 172
[34] Kottmann J P and Martin O J F 2001 *Opt. Lett.* **26** 1096
[35] Maier S A and Harry A A 2005 *J. Appl. Phys.* **98** 011101